Gene Expression **2026** vol. 25(2) | e00089
DOI: 10.14218/GE.2025.00089

Original Article

Analysis of *MIR142* Gene Mutations in Primary Diffuse Large B-cell Lymphoma of the Central Nervous System: A Cross-sectional Study

Elena Voropaeva[1,2*], Olga Seregina[1], Maria Voytko[1], Tatyana Babaeva[1], Vladimir Maksimov[1,2], Yuriy Orlov[3,4*] and Tatyana Pospelova[1,2]

[1]Department of Therapy, Hematology and Transfusiology, Novosibirsk State Medical University of the Ministry of Health of the Russian Federation, Novosibirsk, Russia; [2]Laboratory of Molecular Genetic Research of Therapeutic Diseases, Research Institute of Internal and Preventive Medicine - Branch of the Federal State Budget Scientific Institution «The Federal Research Center Institute of Cytology and Genetics of Siberian Branch of the Russian Academy of Sciences», Novosibirsk, Russia; [3]Chair of information technologies and medical data analysis, Center of Digital Health and AI in medicine, Institute of Digital Biodesign and AI in medicine, Federal State Autonomous Educational Institution of Higher Education I.M. Sechenov First Moscow State Medical University of the Ministry of Health of the Russian Federation, Moscow, Russia; [4]Department of Mechanics and Mathematics, Novosibirsk State University, Novosibirsk, Russia

Received: November 11, 2025 | **Revised:** March 31, 2026 | **Accepted:** April 13, 2026 | **Published online:** April 28, 2026

Abstract

Background and objectives: The pathogenic role of *MIR142* genetic abnormalities in the development of primary diffuse large B-cell lymphoma (DLBCL) of the central nervous system (CNS) is unexplored. The objective of this study was to investigate the frequency, spectrum, and functional significance of mutations in the *MIR142* gene in primary CNS DLBCL.

Methods: Direct Sanger sequencing of the *MIR142* gene was performed in tumor tissue from 35 patients with primary DLBCL of the CNS. *In silico* prediction of microRNA (miRNA)–target interactions, enrichment analysis of target gene ontologies, and prediction of the secondary structure and minimum free energy of the miRNA hairpin were performed.

Results: The mutation frequency was 37.1% (95% confidence interval: 23.2–53.7%). The vast majority of the identified single-nucleotide variants were located outside the regions encoding mature miRNA chains. *In silico* analysis showed that the n.29A>G mutation located in the seed sequence of miR-142-5p resulted in a significant reduction in the number of potential targets and alterations to the interaction spectrum. All single-nucleotide variants identified in the study patients caused a change in minimum free energy and affected the shape and length of the hairpin stem of pri-miRNA. The results indicate the fragility of the pri-miR-142 hairpin.

Conclusions: The frequency of gene mutations in primary DLBCL of the CNS significantly exceeds that reported for systemic DLBCL.

Keywords: Diffuse large B-cell lymphoma; Central nervous system; MicroRNAs; *MIR142* gene; Mutations; Sequencing; Single-nucleotide variants.

[*]**Correspondence to:** Elena Voropaeva, Department of Therapy, Hematology and Transfusiology, Novosibirsk State Medical University of the Ministry of Health of the Russian Federation, Krasny Prospekt 52, Novosibirsk 630091, Russia. ORCID: https://orcid.org/0000-0001-7542-7285. Tel: +7-383-222-22-86, Fax: +7-383-222-22-86, E-mail: vena.81@mail.ru; Yuriy Orlov, Center of Digital Health and AI in medicine, Sechenov First Moscow State Medical University of the Ministry of Health of the Russian Federation, Trubetskaya 8-2, Moscow 119048, Russia, ORCID: https://orcid.org/0000-0003-0587-1609. Tel: +7-495-609-14-00, Fax: +7-499-248-01-81, E-mail: orlov@bionet.nsc.ru

How to cite this article: Voropaeva E, Seregina O, Voytko M, Babaeva T, Maksimov V, Orlov Y, *et al*. Analysis of *MIR142* Gene Mutations in Primary Diffuse Large B-cell Lymphoma of the Central Nervous System: A Cross-sectional Study. *Gene Expr* 2026;25(2):e00089. doi: 10.14218/GE.2025.00089.

Introduction

Diffuse large B-cell lymphoma (DLBCL) is the most common aggressive variant of B-cell non-Hodgkin lymphomas and is characterized by pronounced clinical and molecular heterogeneity among its subtypes. In particular, systemic DLBCL is distinguished by the potential involvement of non-lymphoid organs and tissues in the tumor process, in addition to the lymphatic system, including lesions of the central nervous system (CNS).[1,2] Primary CNS lymphoma (PCNSL) is described as a separate diagnostic form. In the vast majority of cases, it is characterized histologically as DLBCL, is localized in the craniospinal region, and involves the follow-

ing organs (in descending order of frequency of involvement): the brain, eyes, and membranes of the brain and spinal cord, without signs of systemic disease.[3] Accumulated evidence indicates that primary CNS lymphoma is a distinct biological entity and is distinguished from systemic DLBCL, and chronic activation of BCR and NF-κB signaling pathways, in combination with a pronounced ability to evade immune surveillance, plays a crucial role in its development.[4]

PCNSL accounts for 4–6% of extranodal lymphoma variants, up to 1% of all lymphomas, and about 2% of CNS tumors.[4,5] Largely due to improved diagnosis of the disease, the incidence of PCNSL increased threefold between 1973 and 1984. Nevertheless, according to data from the Surveillance, Epidemiology, and End Results database, the incidence rate had stabilized by 2013.[6] At the same time, a continuing gradual increase in the incidence of PCNSL among the elderly has been reported.[7]

Notably, the prognosis of patients with PCNSL is significantly worse than that of patients with secondary CNS involvement in systemic DLBCL. Despite the fact that treatment recommendations are largely based on phase II clinical trials, there is still no consensus regarding the optimal induction regimen in the international medical community. Although induction therapy achieves remission in approximately 50% of patients overall, the risk of relapse remains unacceptably high without subsequent consolidation treatment.[4,8]

Although the traditional diagnosis of PCNSL, based on histomorphological analysis and immunophenotyping of malignant lymphocytes, has been in use for a considerable time, the molecular-level changes due to variations in the genomes, transcriptomes, epigenomes, proteomes, and metabolomes of tumor cells remain poorly understood due to the rarity of this disease. Further advances in understanding the molecular pathogenesis of primary CNS DLBCL are needed, including the identification of biological features and oncogenic pathways that could serve as potential therapeutic targets.[1,9]

In recent years, the diagnostic and prognostic role of microRNAs (miRNAs) in non-Hodgkin lymphomas, and particularly in DLBCL, has been actively studied,[10,11] as well as the molecular mechanisms of their deregulation in these diseases.[12,13]

miRNAs are small regulatory RNA molecules with a length of 18–25 ribonucleotides that regulate gene expression at the post-transcriptional level and are functionally involved in a wide range of biological processes. These endogenous molecules are capable of binding complementarily to the 3′-untranslated regions of target messenger RNA (mRNA), which results in either translational suppression or mRNA cleavage, ultimately leading to decreased levels of the encoded protein and often to changes in intracellular signaling pathways.[14]

miR-142 is considered one of the crucial tumor-suppressive miRNAs in human and animal lymphoid neoplasms. The targets of miR-142-5p and miR-142-3p include a large number of key regulatory genes involved in B-cell lymphopoiesis. According to published studies, this miRNA has a wide range of tumor-suppressive functions by targeting a number of important proto-oncogenes, the dysregulation of which contributes to increased proliferation, inhibition of apoptosis, activation of B-lymphocyte survival signaling pathways, metabolic reprogramming, creation of an immunosuppressive microenvironment and immune evasion, as well as tumor cell dissemination.[15]

There are a number of important observations regarding the features of miR-142 expression in systemic DLBCL. Firstly, it was found that the level of this miRNA in primary samples of patients with DLBCL is significantly higher than in Burkitt lymphoma samples and in healthy lymphoid tissue.[16,17] Secondly, miRNA profiling in DLBCL cell lines U2932 and SUDHL5 showed high levels of both miR-142-3p and miR-142-5p in the total miRNA pool, as well as their significant enrichment in association with the Ago-2 protein as part of the RISC complex. These findings allow both mature strands to be considered biologically highly active in the analyzed cells.[18,19] Thirdly, the expression level of miR-142 in DLBCL, determined by next-generation sequencing methods, is characterized by pronounced heterogeneity, with low expression of miR-142 associated with higher survival rates in DLBCL patients receiving therapy according to the R-CHOP protocol.[20,21] Finally, it was found that the mutational status of the *MIR142* gene (OMIM, https://www.omim.org/entry/615657) was observed in systemic DLBCL at a notably high frequency, ranging from 12% to 20%.[22–25] No other variant of hematological malignancies or solid tumors has revealed equally frequent mutations in *MIR142* or any other miRNA genes.[19] Despite this, the pathogenic role of molecular genetic alterations in miR-142 and the *MIR142* gene in the development of primary CNS DLBCL remains largely unstudied.

The objective of this study was to investigate the frequency, spectrum, and functional significance of mutations in the *MIR142* gene in primary CNS DLBCL.

Materials and methods

Tumor samples and DNA isolation

The set of materials was collected at the Novosibirsk Regional Center of High Medical Technologies from 2015 to 2019. The following inclusion criteria were used: consent to be included in the study; primary cases of CNS lymphomas without prior treatment; an isolated tumor lesion of the CNS without systemic manifestations; and histological and immunohistochemical confirmation of diffuse large B-cell lymphoma as the tumor subtype. The exclusion criteria were: refusal to be included in the study; secondary involvement of the CNS in lymphoma; and histological and immunohistochemical verification of a tumor variant other than diffuse large B-cell lymphoma. All eligible cases were included (Fig. 1).

Archived FFPE blocks of biopsies obtained by stereotactic biopsy of tumor foci from 35 patients with PCNSL were examined. Table 1 contains the characteristics of the study subjects. In accordance with the criteria of the current classification of the World Health Organization and using histological and immunohistochemical studies, the histological variant of PCNSL was identified as diffuse large B-cell lymphoma in all patients.[26] The study was approved by the Bioethics Committee of Novosibirsk State Medical University (№129 from November 30, 2020) and was conducted in compliance with the Declaration of Helsinki (as revised in 2024). Written informed consent was obtained from all study participants. DNA was extracted by the phenol-chloroform method with guanidine.

The assessment of MIR142 gene sequencing

The coding region of the *MIR142* gene with adjacent regions was amplified using the 5′-CTCACCTGTCACACGAGGTC-3′ and 5′-CTCTTGAGCAGGAGGTCAGG-3′ primers.[27] A 231 bp product was obtained, including the full-length pri-miR-142 transcript with flanking regions (Fig. 2).

After purification, the product was subjected to direct capillary sequencing using the BigDye Terminator v3.1 Cycle Sequencing Kit and POP-7 polymer (Applied Biosystems, USA) on an ABI

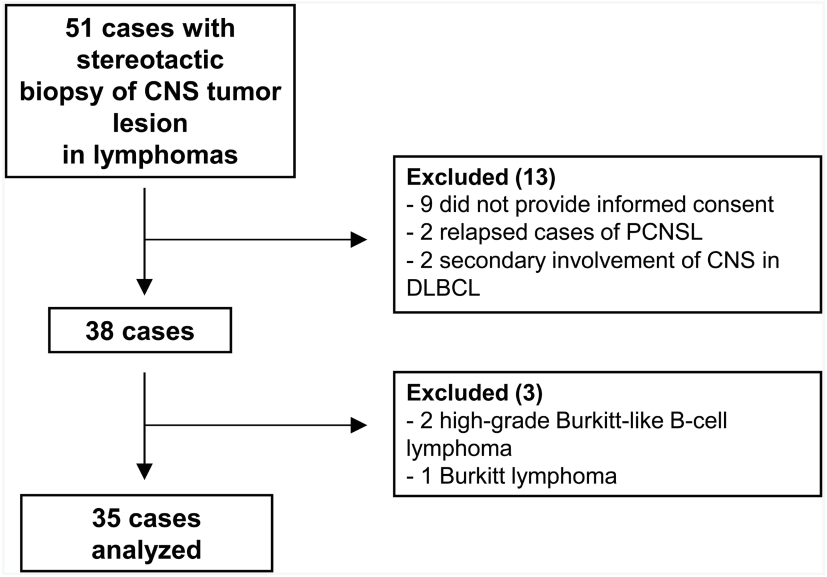

Fig. 1. Flow diagram detailing patient selection, inclusion, and exclusion. CNS, central nervous system; DLBCL, diffuse large B-cell lymphoma; PCNSL, primary CNS lymphoma.

3500 genetic analyzer (Applied Biosystems, USA). The obtained sequence chromatograms were analyzed using Chromas software.

The detected nucleotide sequence variants were specified according to the Human Genome Variation Society nomenclature and in relation to the nucleotide numbering in miRNA precursors, as deposited in miRBase release 22.1.[28,29]

Statistical and in silico analysis

Mutation frequencies are described as absolute and relative frequencies with 95% confidence intervals (95% CI) using the Wilson method.

The UNAFold web server (https://www.unafold.org/) was used to predict the secondary structure of the miRNA hairpin and calculate its minimum free energy (MFE). The medians and the 25th and 75th percentiles of MFE were calculated (Me (Q25; Q75)). The Mann–Whitney test was used to assess the statistical significance of differences in MFE between groups. Differences were considered statistically significant at $P < 0.05$.

In silico prediction of target genes for each of the seed miRNA sequences was performed using the miRDB online tool.[30]

To determine the function of miRNA target genes, an enrichment analysis of gene ontology terms (Gene Ontology (GO) enrichment analysis) of molecular functions and biological processes was carried out using PANTHER based on the GO bioinformatics resource (http://www.geneontology.org).[31,32] Results with a *P*-value < 0.05 after adjustment for multiple hypothesis testing (FDR—false discovery rate) were considered statistically significant.

Results

The frequency of mutations in the MIR142 gene in PCNSL

In the studied group of tumor tissue samples from patients with PCNSL, 14 types of single nucleotide substitutions (SNVs) in the *MIR142* gene were identified in one-third of cases (13 out of 35, 37.1%, 95% CI (23.2; 53.7)) (Table 2, Fig. 3). Two SNVs were detected simultaneously in three samples, and three SNVs were found in one sample. Positions n.20, n.89, n.93, and n.95 underwent recurrent changes.

More than half (10/18, 55.6%, 95% CI (33.7; 75.4)) of the identified SNVs were transversions (substitutions of the C–G, T–A, and A–C types), while the rest (8/18, 44.4%, 95% CI (24.6; 66.3)) were transitions (C–T and G–A), which usually occur only in cases with multiple mutations.

Analysis of the distribution of SNVs showed that the overwhelming majority (13/18, 72.2%, 95% CI (49.1; 87.5)) were located outside the regions encoding mature miRNA chains, namely in pri-miR-142. Only 5/18 (27.8%, 95% CI (12.5; 50.9)) affected the sequence of mature miRNA miR-142-5p, and one SNV (5.6%, 95% CI (1.0; 25.8)) was located in the seed sequence (Fig. 4a).

Results of the pri-miR-142 hairpin thermodynamic stability and secondary structure analysis

The UNAFold web server was used to assess the impact of the identified SNVs on the thermodynamic stability and secondary structure of the pri-miR-142 hairpin. Under normal conditions, MFE of the predicted secondary structure of the miRNA precursor hairpin was −44.9 kcal/mol. According to *in silico* prediction, sequence alterations in the coding region of the *MIR142* gene led to changes in the minimum free energy (ΔMFE), ranging from 0.8 to 8.4 kcal/mol in absolute terms (Fig. 4b). In 10 out of 13 cases (76.9%), the mutations increased the MFE, resulting in less negative values (Me = −41.0 (−41.1; −39.7) kcal/mol), indicating reduced thermodynamic stability, whereas in the remaining cases (3/13, 23.1%), the mutations decreased the MFE, resulting in more negative values (Me = −48.8 (−49.1; −47.7) kcal/mol), indicating increased thermodynamic stability. These differences were statistically significant compared with cases without mutations in the *MIR142* gene ($P < 0.001$ and $P = 0.001$, respectively).

The data on the predicted structure of the hairpin of normal pri-miR-142 (Fig. 5a)[33,34] and pri-miR-142 with the identified SNVs (Supplementary Fig. 1) are noteworthy. As shown in Table 3, there are changes in stem length and the number of unstructured elements (such as mismatches and bubbles in the stem), as well as dis-

Table 1. Baseline characteristics of the study subjects

Case	Sex	Age	Lesions		Immunophenotype	Stage
			Locus	Number		
PCNSL1	F	65	B	Multiple	DLBCL	IV
PCNSL2	F	69	B	Solitary	DLBCL	IV
PCNSL3	M	66	B	Solitary	DLBCL	IV
PCNSL4	M	72	B	Multiple	DLBCL	IV
PCNSL5	F	49	B	Multiple	DLBCL	IV
PCNSL6	F	70	B+SC	Multiple	DLBCL	IV
PCNSL7	M	64	B	Solitary	DLBCL	IV
PCNSL8	M	48	B	Multiple	DLBCL	IV
PCNSL9	M	54	B	Multiple	DLBCL	IV
PCNSL10	M	72	B	Solitary	DLBCL	IV
PCNSL11	F	55	B	Solitary	DLBCL	IV
PCNSL12	F	62	B	Solitary	DLBCL	IV
PCNSL13	F	73	B	Multiple	DLBCL	IV
PCNSL14	M	33	B	Solitary	DLBCL	IV
PCNSL15	F	53	B	Multiple	DLBCL	IV
PCNSL16	F	61	SC+NL	Solitary	DLBCL	IV
PCNSL17	F	18	B+NL	Solitary	DLBCL	IV
PCNSL18	F	54	B	Solitary	DLBCL	IV
PCNSL19	M	50	B	Solitary	DLBCL	IV
PCNSL20	M	54	B	Solitary	DLBCL	IV
PCNSL21	M	36	SC+NL	Solitary	DLBCL	IV
PCNSL22	M	50	B	Multiple	DLBCL	IV
PCNSL23	M	61	B	Multiple	DLBCL	IV
PCNSL24	F	43	B	Solitary	DLBCL	IV
PCNSL25	F	59	B+NL	Solitary	DLBCL	IV
PCNSL26	M	62	B	Solitary	DLBCL	IV
PCNSL27	M	53	B	Multiple	DLBCL	IV
PCNSL28	F	62	B	Solitary	DLBCL	IV
PCNSL29	M	62	B	Multiple	DLBCL	IV
PCNSL30	M	57	B	Solitary	DLBCL	IV
PCNSL31	M	72	B	Multiple	DLBCL	IV
PCNSL32	M	67	B	Solitary	DLBCL	IV
PCNSL33	M	27	B+NL	Solitary	DLBCL	IV
PCNSL34	F	37	B	Multiple	DLBCL	IV
PCNSL35	M	73	B	Solitary	DLBCL	IV

B, brain; DLBCL, diffuse large B-cell lymphoma; F, female; M, male; NL, neuroleukemia; PCNSL, primary CNS lymphoma; SC, spinal cord.

ruption of main functional motifs in the majority of cases: destruction of mismatched GHG on the 3′ strand 7–9 nucleotides from the basal junction (n.20G/C); changes in the secondary structure in the CNNC motif downstream of the basal junction (n.95G/U, n.100C/U, n.101U/G); lengthening (n.100C/U) or reduction (n.97G/A, n.95G/U) of stem length due to changes in the location of the basal junction; reduction of single-stranded segments at the base of the stem (n.100C/U, n.101U/G); destruction of the base-paired stable platform in the basal stem (n.93C/G); and changes in the secondary structure in the mismatched GHG on the 3′ strand 7–9 nucleotides from the basal junction (n.89U/A).

Changes in the profile of predicted miRNA–target interactions as a result of seed sequence mutation

Considering that the n.29A/G substitution affected the seed sequence of mature miR-142-5p, the identification of target gene sets in the normal gene and its mutant variant was carried out using the miRDB service.[30] The analysis revealed a change in the profile of predicted miRNA–target interactions (Fig. 5b). In the case of n.29A/G in the key miR-142-5p sequence, there was a decrease from 1,133 to 599 in the number of potential targets and a significant change in the interaction spectrum compared to the normal sequence. With this mutation, control was retained over only 79/1,133 (6.8%), while 1,054/1,133 (93.2%) canonical mRNA targets were lost; meanwhile, 520 out of 599 (86.8%) predicted interactions of the analyzed mutant variant of the seed miR-142-5p sequence were new.

The next step was to perform an enrichment analysis of gene ontology terms of biological processes for each of the target gene sets. The analysis revealed statistically significant ($P < 0.05$) enrichment of different sets of gene ontology terms for normal miR-142-5p and the n.29A/G substitution (Supplementary Fig. 2).

There was a loss of control over targets involved in regulation of gene expression (GO:0010468), cell death (GO:0008219), cell differentiation (GO:0030154), cell migration (GO:0016477), chromatin organization (GO:0006325), chromatin remodeling (GO:0006338), intracellular signal transduction (GO:0035556), maintenance of cell number (GO:0098727), regulation of canonical NF-κB signal transduction (GO:0043122), regulation of cell adhesion (GO:0030155), regulation of the cell cycle (GO:0051726), regulation of cellular response to growth factor stimulus (GO:0090287), vesicle-mediated transport (GO:0016192), and many others. Some specific key target genes are listed in Table 4.

Discussion

The descriptions of mutations in the *MIR142* gene identified in chronic lymphoid leukemia,[35] acute myeloid leukemia, and myelodysplastic syndrome,[36,37] and in isolated cases of follicular lymphoma and myeloproliferative diseases are contained in modern literature.[23,27,38] Taking into account all hematological malignancies, mutations in *MIR142* are most often detected in systemic DLBCL.[19]

The frequency and spectrum of SNVs in the *MIR142* gene in tumor tissue of 35 cases of primary CNS DLBCL were characterized in detail for the first time, and an *in silico* analysis of their functional effect was performed in this study. The frequency of SNVs in the study group was 37.1%, which exceeds the frequency described in the literature for systemic DLBCL, ranging from 12% to 20%.[22–25]

It is important to note that there were multiple SNVs in the gene sequence in one third of the cases in our study. The study, performed using NGS methods, showed an extremely high frequency of kataegis in the region of the *MIR142* gene in systemic DLBCL.[39] Kataegis is described as an occurrence of somatic hypermutations in a number of malignant neoplasms characterized by clusters (six

TTGGGGGGAT CTTAGGAAGC CACAAGGAGG GCTGGGGGGC TCTTGGAGCA
GGAGTCAGGA GGCCTGGGCA GCCTGAAGAG TACACGCCGA CGGACAGACA
GACAGTGCAG TCACCCATAA AGTAGAAAGC ACTACTAACA GCACTGGAGG
GTGTAGTGTT TCCTACTTTA TGGATGAGTG TACTGTGGGC TTCGGAGATC
ACGCCACTGC TGCCGCCCGC TGCCCGCCAC CATCTTCCTC GGCGCTCGGG
GACCTCGTGT GACAGGTGAG CACCTTACGG CCCCTCC

Fig. 2. The sequence of the *MIR142* gene. The primer annealing sites are marked in green. The underscore indicates the pri-miR-142 sequence, while the pre-miR-142 sequence is highlighted in bold.

or more within a thousand bp) of one type of replacement, about 70% of which are represented by transitions of type C>T.[40] All of them are localized on one of the DNA strands and appear as a result of deamination of cytidine during the repair of double-stranded breaks when DNA is in a single-stranded state.[41] Since we analyzed a relatively small portion of the nucleotide sequence using the Sanger direct capillary sequencing method, this does not allow us to assess the allelic location of the identified substitutions and confirm the high incidence of kataegis in our study. Supplementary NGS analysis of a subset of samples to assess mutation density within the *MIR142* locus (e.g., mutations per 1000 bp) would strengthen this claim. However, kataegis can be inferred from the fact that cases with multiple mutations were characterized by transitions, including repeated substitutions of G>A, which are typical for this mutagenesis mechanism. There is also evidence of sustained activation-induced cytidine deaminase expression in a fraction of PCNSL in published data.[4]

A total of 18 SNVs scattered across the gene sequence were detected in the tumor tissue of primary CNS DLBCL in our study. These findings are a hallmark of this disease, distinguishing it from other types of hematological malignancies. Thus, according to current published data, all currently known SNVs in this gene in acute myeloid leukemia and myelodysplastic syndrome have been described only in the 'seed' region of the mature miR-142-3p chain, which is responsible for binding to targets,[36,37,42,33] as well as the only currently described mutation in *MIR-142* in Burkitt's lymphoma.[43] The verified SNVs affect the miR-142-3p sequence in follicular lymphoma,[23,38] and in the vast majority of cases of chronic lymphocytic leukemia they are located in miR-142-5p.[27,35,33] However, the pattern of SNV distribution in

Table 2. Characteristics of mutations in *MIR142* identified in the study group (MFE means the minimum free energy)

Sample	Coordinates according GRCh38.p14 (MAF in GnomAD_exomes)	dbSNP IDs	Mutations pri-miR-142		Location	MFE, kcal/mol
			DNA	RNA		
Normal	-	-	-	-	-	−44.9
PCNSL1	chr17:58331316 G>A (−)		n.13C/T	n.13C/U	pri-miR-142	−36.5
	chr17:58331300 T>C (−)	rs867010562	n.29A/G	n.29A/G	seed sequence miR-142-5p	
	chr17:58331293 T>C (−)		n.36A/G	n.36A/G	miR-142-5p	
PCNSL2	chr17:58331309 C>G (−)		n.20G/C	n.20G/C	pri-miR-142	−39.5
	chr17:58331294 C>T (0.000003)	rs1441344858	n.35G/A	n.35G/A	miR-142-5p	
PCNSL3	chr17:58331234 C>T (−)		n.95G/A	n.95G/A	pri-miR-142	−40.2
	chr17:58331232 C>T (−)		n.97G/A	n.97G/A	pri-miR-142	
PCNSL4	chr17:58331234 C>A (−)		n.95G/T	n.95G/U	pri-miR-142	−41.4
	chr17:58331216 G>C (0.000068)	rs578020025	n.113C/G	n.113C/G	-	
PCNSL5	chr17:58331289 G>A (0.000005)	rs1240205037	n.40C/T	n.40C/T	miR-142-5p	−39.2
PCNSL6	chr17:58331309 C>G (−)		n.20G/C	n.20G/C	pri-miR-142	−48.8
PCNSL7	chr17:58331229 G>A (−)		n.100C/T	n.100C/U	pri-miR-142	−49.3
PCNSL8	chr17:58331236 G>C (−)	rs1567856421	n.93C/G	n.93C/G	pri-miR-142	−41.0
PCNSL9	chr17:58331236 G>C (−)	rs1567856421	n.93C/G	n.93C/G	pri-miR-142	−41.0
PCNSL10	chr17:58331240 A>T (−)		n.89T/A	n.89U/A	pri-miR-142	−41.1
PCNSL11	chr17:58331240 A>T (−)		n.89T/A	n.89U/A	pri-miR-142	−41.1
PCNSL12	chr17:58331234 C>A (−)		n.95G/T	n.95G/U	pri-miR-142	−41.6
PCNSL13	chr17:58331228 A>C (0.000006)	rs1486384342	n.101T/G	n.101U/G	pri-miR-142	−46.5

MAF, minor allele frequency; MFE, , minimum free energy; PCNSL, primary CNS lymphoma.

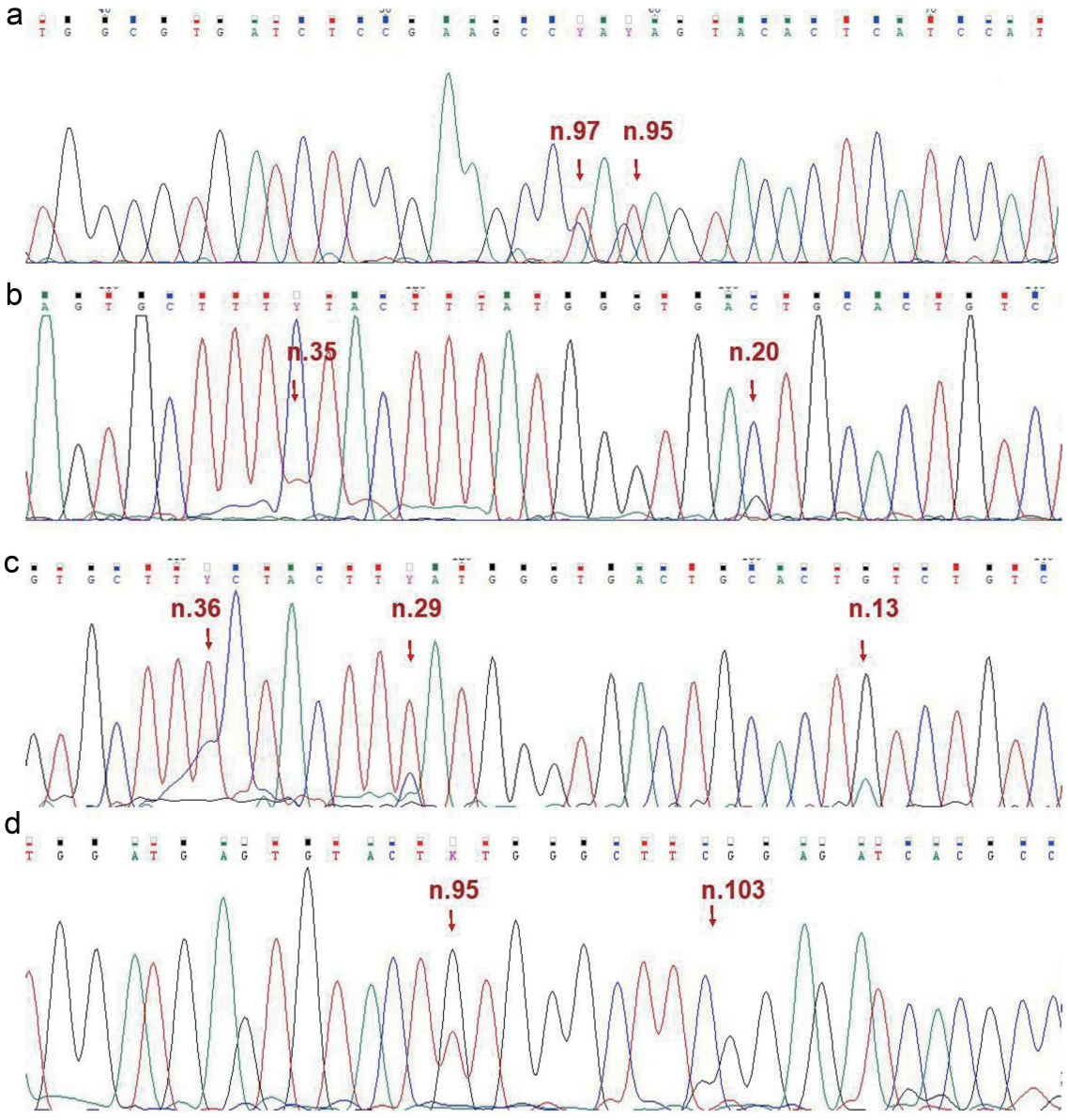

Fig. 3. Fragments of the sequence chromatogram obtained using a reverse primer of DNA samples containing mutations n.95G/A and n.97G/A (a); n.20G/C and n.35G/A (b); n.13C/T, n.29A/G and n.36A/G (c); and fragment of the sequence chromatogram obtained using a forward primer of a DNA sample containing mutations n.95G/T and n.113C/G (d) in the *MIR142* gene.

primary DLBCL of the CNS is not identical to systemic DLBCL (Fig. 5c). Unlike in systemic DLBCL, in which SNVs are scattered across the gene sequence and are often detected in miR-142-3p, including the seed sequence, in primary DLBCL of the CNS they overwhelmingly affect areas involved in the formation of the pri-miR-142 hairpin base. Only 16.7% changed the sequence of the mature miR-142-5p, and only one (5.6%) affected the seed sequence of miR-142-5p.

Our results are consistent with published data indicating an increased frequency of SNVs in miRNA genes in malignant neoplasms, with a distribution pattern shifting from the 'seed' region and mature strand toward the precursor miRNA sequences. This is believed to be associated with a selection process in the tumor favoring functionally significant substitutions.[44]

It is known that SNVs located in the sequence of the miRNA precursor have a profound effect on miRNA functioning, from the nuclear and cytoplasmic stages of their maturation to thermodynamic stability, the formation of secondary structure, and the selection of chains included in RISC, which ultimately affects their expression and functional activity.[45,46]

Using the UNAFold web server, we determined the most stable secondary conformation of the "hairpin" miRNA in thermodynamic equilibrium and its MFE, which depend on factors such as the length of the molecule, the composition of nucleotides, and the sequence of their location in the chain. MFE can be calculated by adding the free energies of complementary interacting base pairs, bulges, and loops. It is noteworthy that the most structured and stable in a series of miRNAs of the same size is considered to be

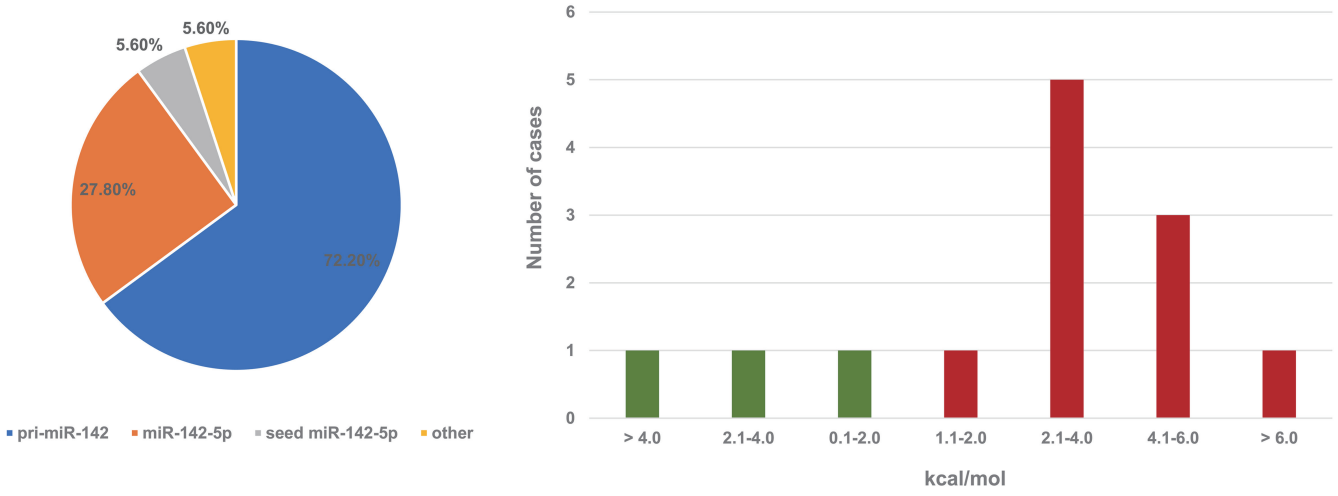

Fig. 4. Number of SNVs identified in various regions of the *MIR142* gene transcript (a) and distribution of absolute changes in hairpin minimum free energy (ΔMFE, kcal/mol): green columns indicate decreased MFE values, i.e., more negative MFE and increased thermodynamic stability; red columns indicate increased MFE values, i.e., less negative MFE and reduced thermodynamic stability (b). MFE, minimum free energy; SNVs, single nucleotide substitutions.

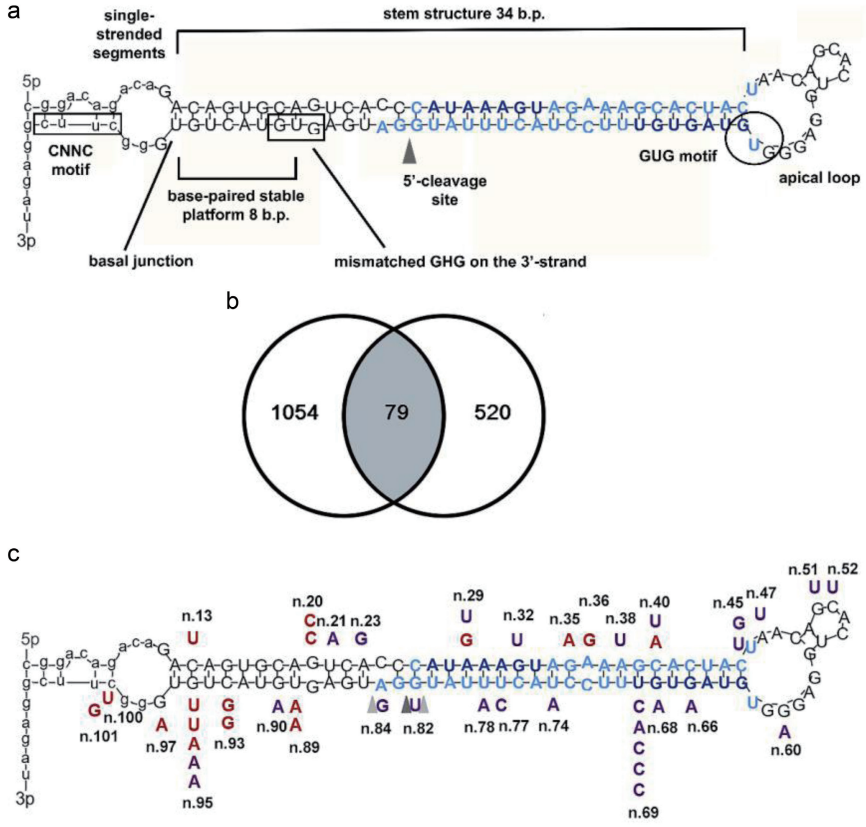

Fig. 5. Secondary structure of the normal pri-miR-142 hairpin (a); Venn diagrams of changes in the target spectrum predicted for microRNAs in normal conditions (left circle) and with n.29A/G in the "seed" sequence of miR-142-5p (right circle); the number of common targets is indicated in the area of intersection of the two circles (b); location of the *MIR142* gene mutations on the predicted secondary stem-loop structure of the wild-type pri-miR-142, modeled using the UNAFold web server (c). Mutations identified in primary CNS lymphoma in our study are shown in red, while mutations in systemic DLBCL reported by Huang *et al*.[33] are shown in purple. Locations of the mutations on the secondary pri-miR-142 stem-loop structure are indicated by nucleotide position numbers. The sequence of mature microRNA strands is indicated in blue, with the "seed sequences" of miR-142-5p and miR-142-3p highlighted in dark blue. Flanking regions and the terminal loop are shown in black. The dark gray triangle marks the position of the original dominant DROSHA cleavage site, and light gray triangles indicate additional cleavage sites according to Ma *et al*.[34] CNS, central nervous system; DLBCL, diffuse large B-cell lymphoma.

Table 3. Key structural effects of *MIR142* mutations identified in the study group on pri-miR-142 hairpin structure

Sample	Key structural effects
PCNSL1	
n.13C/U	"Seed" sequence changes
n.29A/G	
n.36A/G	
PCNSL2	
n.20G/C	Destruction of mismatched GHG on the 3′ strand 7–9 nucleotides from the basal junction
n.35G/A	
PCNSL3	
n.95G/A	Reduction of the stem length by changing the location of the basal junction
n.97G/A	
PCNSL4	
n.95G/U	Changes in the secondary structure in the CNNC motif downstream of the basal junction, reduction of the stem length by changing the location of the basal junction
n.113C/G	
PCNSL5	
n.40C/T	No data
PCNSL6	
n.20G/C	Destruction of mismatched GHG on the 3′ strand 7–9 nucleotides from the basal junction
PCNSL7	
n.100C/U	Destruction of the CNNC motif and changes in the secondary structure downstream of the basal junction, lengthening of the stem length by reduction of the single-stranded segments at the base of the stem
PCNSL8	
n.93C/G	Destruction of the base-paired stable platform in the basal stem
PCNSL9	
n.93C/G	Destruction of the base-paired stable platform in the basal stem
PCNSL10	
n.89U/A	Changes in the secondary structure in the mismatched GHG on the 3′ strand 7–9 nucleotides from the basal junction
PCNSL11	
n.89U/A	Changes in the secondary structure in the mismatched GHG on the 3′ strand 7–9 nucleotides from the basal junction
PCNSL12	
n.95G/U	Changes in the secondary structure in the CNNC motif downstream of the basal junction, reduction of the stem length by changing the location of the basal junction
PCNSL13	
n.101U/G	Changes in the secondary structure in the CNNC motif downstream of the basal junction, reduction of the single-stranded segments at the base of the stem

PCNSL, primary CNS lymphoma.

the one with the highest negative value of MFE.[47]

The analysis showed that all SNVs identified in the study group resulted in changes in MFE in the range from 0.8 to 8.4 kcal/mol in absolute terms. In most cases (76.9%), the SNVs increased the MFE, making the predicted hairpin structure less negative and, consequently, less thermodynamically stable, while the rest (23.1%), according to the prediction of the UNAFold web server, stabilized the secondary structure of the molecule. It is worth noting that Gong *et al*.[48] summarized the existing studies in this area and found that changes in MFE by more than 2.0 kcal/mol significantly affect the production of mature miRNA, but even changes below this threshold can alter their biogenesis.[49]

More recently, the thermodynamic properties of the hairpin have been shown to determine the functionality of the molecule, affecting the rate and selectivity of inclusion of a particular mature chain into RISC, as well as its dissociation from the target after

Table 4. Key predicted targets affected by the n.29A/G mutation in *MIR142* gene

Targets	microT score*	TarBase confirmation#	Function
MAPK signaling pathway			
MAP3K2	0.93	Yes	MAP3K2 is a serine/threonine kinase that acts as a key, upstream regulatory node in the MAPK signaling cascade
MAPK9	0.96	No	MAPK9 acts as an integration point for cellular signals, particularly in response to cytokines
MAPK10	0.60	Yes	MAPK10 is a protein kinase that is activated by cytokines
PI3K-AKT-mTOR signaling pathway			
PIK3CA	0.86	Yes	The p110-alpha catalytic subunit of the PI3K enzyme, which is crucial for cellular signaling and drives key cellular processes, including growth, proliferation, metabolism and survival
RICTOR	0.82	Yes	RICTOR is a critical component and scaffolding protein for the mTORC2 complex, essential for its stability, assembly, and function. It regulates cell survival, metabolism, proliferation, cytoskeletal reorganization, and metastasis
NF-kB signaling pathway			
TNFSF13B	0.86	Yes	TNFSF13B promotes both canonical and non-canonical NF-kB signaling
JAK-STAT signaling pathway			
IL22	0.87	No	IL-22 acts as a pro-tumorigenic cytokine in lymphomas by driving tumor growth, cell survival and migration, promoting the expression of anti-apoptotic (e.g., Bcl-2, Bcl-XL) and pro-proliferative (e.g., cyclin D1, c-Myc) genes
IL6ST	0.93	Yes	IL6ST encodes the GP130 protein, which transduces the proinflammatory signaling of the IL6 cytokine family
Critical cell surface adhesion molecules mediating cell–cell and cell–matrix interactions			
ALCAM	0.83	Yes	ALCAM is a cell adhesion molecules involved in the interaction with the vascular endothelium and migration of B-lymphocytes across the blood-brain barrier
ITGAV	1.00	Yes	ITGAV acts as a key mediator of CNS tumor neoangiogenesis and immune checkpoint blockade
ITGAM	0.62	Yes	ITGAM is associated with immune checkpoint blockade
ITGA9	0.69	Yes	ITGA9 is closely related to the proliferation, metastasis, adhesion, and angiogenesis of tumor cells
Immunity checkpoints			
CD47	0.44	Yes	CD47 is a membrane glycoprotein (“don’t eat me signal”) expressed on cells that prevents their destruction by macrophages by interacting with the SIRPα receptor
CD109	0.98	Yes	CD109 orchestrates reprogramming of tumor-associated macrophages to dampen immune response
Cell cycle and apoptosis			
MCL1	0.85	Yes	MCL1 is an antiapoptotic protein from the BCL-2 family, encoded by the gene of the same name, which prevents cell death by binding proapoptotic proteins (BAK, BAX)
MDM4	0.92	Yes	MDM4 acts as a key negative regulator of the tumor suppressor p53
PKN2	0.79	Yes	PKN2 plays a role in the regulation of cell cycle progression, actin cytoskeleton assembly, cell migration, cell adhesion, tumor cell invasion and transcription activation signaling processes
CCNH	0.79	Yes	CCNH plays a key role in the activation of CDK kinases (CDK1, 2, 4, 6) of the cell cycle

*According to the DIANA-microT 2023 algorithm, which provides microT-CDS interaction scores to predict microRNA binding; #The database of experimentally supported microRNA targets on protein-coding transcripts. ALCAM, activated leukocyte cell adhesion molecule, CNS, central nervous system.

silencing.[50] In addition, mutations outside the seed sequence can alter the efficiency of miRNA inclusion in the RISC complex, as well as potentially disrupt interactions with RNA sponges that adsorb miRNAs and thus suppress their activity.[50–54]

Thus, most of the SNVs identified in this study are located outside the seed sequences and, at first glance, do not appear to have a direct impact on the choice of miRNA target gene. However, beyond thermal stability, great attention should be drawn to the secondary conformation of the miRNA hairpin. The obtained data may indicate that the pri-miR-142 hairpin has a fragile structure.

As can be seen from Supplementary Figure 1, in most cases the detected SNVs, according to *in silico* prediction, cause a significant change in the shape and length of the pri-miRNA hairpin stem. This is significant for the first stage of miRNA biogenesis, namely, the processing of pri-miRNA by the Drosha–DGCR8 complex.

Currently, there is no complete understanding of how the microprocessor recognizes pri-miRNAs and orients itself asymmetrically on the stem-loop structure to select the correct cleavage site. The following model has been proposed: interaction of DGCR8 at the apical loop provides effective cleavage by orienting Drosha toward the basal stem. Thus, both the basal and apical junctions cooperatively coordinate cleavage position and processing efficiency. Structural features are of prime importance in defining how efficiently a pri-miRNA is recognized and processed by the microprocessor.[55]

Recent research has revealed two important findings. Firstly, the distances from both the lower and upper junctions of the pri-miRNA stem to the single-stranded regions of the molecule in human cells play an important role in determining the cleavage site. If these distances are suboptimal, Drosha–DGCR8 may cleave pri-miRNA at non-canonical sites.[34]

Secondly, while the 3′ ends of most miRNAs tend to exhibit variability, the 5′ ends of mature miRNAs are typically highly conserved. This is because nucleotides 2 through 8 comprise the seed sequence, which is critical for target recognition.[56] Consequently, even a single-nucleotide shift in the pri-miRNA stem length in either direction can disrupt the coordination of Drosha–DGCR8 processing, leading to alternative cleavage and the emergence of different miRNA-5p variants with distinct seed sequences and different target gene pools. It is therefore hypothesized that SNVs located within regions forming the basal part of the pri-miR-142 hairpin may impair Drosha–DGCR8 processing accuracy, resulting in the generation of non-canonical miR-142-5p isoforms and potentially altering its target gene repertoire in CNS-type DLBCL.

The predicted normal pri-miR-142 hairpin structure in our study has key functional elements necessary for processing by the Drosha–DGCR8 complex: a stem of about 33–35 nucleotides long, an apical loop of 10–15 nucleotides with a GUG motif, single-stranded segments at the base of the stem, a CNNC motif downstream of the basal junction, a mismatched GHG motif on the 3′ strand 7–9 nucleotides from the basal junction (in which H is any nucleotide but G), a base-paired stable platform in the basal stem, and a 5′ cleavage site at nucleotide positions 14–15 from the basal junction (Fig. 5a). The primary sequence of all of these motifs has an additive effect on efficient processing. It is known that changes in the length of the stem and the number of unstructured elements (such as mismatches and bubbles on the stem), as well as disruption of main functional motifs, affect the efficiency and accuracy of processing.[54]

Thus, it is assumed that SNVs located in the sequence regions involved in the formation of the pri-miR-142 hairpin base may impair the cleavage process by the Drosha–DGCR8 complex, resulting in the formation of non-canonical variants of miR-142-5p and changing the pool of target genes of mature miR-142-5p in DLBCL. According to Fukunaga *et al*.,[57] 5′-isomers can also be generated by non-canonical binding of the Dicer protein to pre-miRNA.

It was found that the canonical miR-142-5p variant potentially targets 1,133 mRNAs.[30] We performed a bioinformatic analysis of the effect of n.29A/G in the *MIR142* gene on the switching of miR-142-5p target genes, which showed that this SNV leads to a significant change in the set of regulated genes, namely a halving of the number of potential targets (to 599) and a significant change in the spectrum of interaction. According to *in silico* analysis, control was retained over only 6.8% of canonical mRNA targets, while 93.2% of them were lost. Notably, 86.8% of the predicted interactions of the analyzed mutant variant of the miR-142-5p seed sequence were novel. These changes were directly reflected in the results of GO term enrichment analysis for the obtained gene lists. The GO enrichment results indicate loss of control over tumor-related pathways: regulation of gene expression, cell death, cell differentiation, cell migration, chromatin organization, chromatin remodeling, intracellular signal transduction, maintenance of cell number, regulation of canonical NF-κB signal transduction, regulation of cell adhesion, regulation of cell cycle, regulation of cellular response to growth factor stimulus, vesicle-mediated transport, and many others.

Thus, targeting of common anti-apoptotic proteins (MCL1 and MDM4) and cell cycle promoters (PKN2 and CCNH) is violated in tumors. In particular, MCL1 and MDM4 are deregulated in a significant fraction of ABC DLBCLs (the predominant subtype in PCNSL) and contribute to therapy resistance.[58,59]

The following is a discussion of some critical deregulated targets as a result of the mutation n.29A/G in the *MIR142* gene, which are not only predicted in our work, but also have experimental evidence of interaction with miRNAs and are presented in the TarBase database.[60]

The origin of tumor cells in PCNS remains unclear. It is most likely that this tumor arises from transformed peripheral B lymphocytes that have escaped immune surveillance and hidden in the CNS. To do this, they overcome the blood-brain barrier, the densest blood-tissue barrier, and then survive and proliferate in an extremely poor growth-stimulus environment of the CNS. The currently accumulated data indicate that the following mechanisms play a central role in the development of a tumor: adhesion and extravasation, cell signaling, autocrine stimulation, induction and maintenance of inflammation, activation of neoangiogenesis, and escape of immune surveillance.[5]

The following immune escape molecules are noteworthy. Recently, several studies have reported increased CD47 expression on lymphoma cells of different types. Binding of CD47 on tumor lymphocytes to SIRPα suppresses the phagocytic function of macrophages and enables avoidance of control by innate immunity.[61] Treatments that block the interaction of CD47 and SIRPα significantly suppress tumor growth and metastasis through diverse mechanisms, such as phagocytosis, antibody-dependent cellular cytotoxicity, and apoptosis.[62,63] CD47 expression is frequent in ABC and a subset of GCB DLBCL with mutations in *TP53* and/or *CCND1*, and is related to tumor-associated macrophage infiltration and disease progression. For these reasons, CD47 is a potential target for the treatment of DLBCL, especially for relapsed and refractory cases.[64] The results of a recent study confirmed the critical role of macrophages and CD47 in controlling PCNSL cell growth.[65,66]

In turn, CD109 orchestrates reprogramming of tumor-associated macrophages to dampen immune response. Moreover, expression of CD109 is a mechanism of down-regulation of TGF-β receptor on lymphoma cells. TGF-β suppresses lymphoma growth by apoptosis and inhibiting proliferation.[67,68]

Another mechanism of evading the immune response by tumor cells is the loss or decrease in the expression of molecules of the major histocompatibility complex class II (MHC-II) as a result of overexpression of NFX1.[69] NFX1 is a nuclear transcription factor,

which downregulates MHC II antigen expression.[70] MHC-II presents antigens to $CD4^+$ T helper cells, and their suppression reduces antitumor immunity, correlating with a worse prognosis and low effectiveness of immunotherapy in many cancers.[71] Unfortunately, interaction of miR-142-5p with NFX1 is currently not recorded in the TarBase and requires experimental confirmation.

PCNSL refers to lymphomas of immune-privileged sites. The development of this tumor requires that neoplastic cells overcome the blood-brain barrier. This may be facilitated by the loss of control over the following targets: ITGAV, ITGAM, ITGA9, and ALCAM. These proteins are key cell adhesion molecules involved in immune response, tumor progression, and cell signaling.

ALCAM (CD166) plays a key role in the pathogenesis of PCNSL, namely in the interaction with the vascular endothelium and migration of B-lymphocytes across the blood-brain barrier. Also, ALCAM expression is considered one of the key factors that ensures the ability of DLBCL cells to survive and proliferate in the immune-privileged environment of the CNS.[39,72] ITGAV acts as a key mediator of CNS tumor neoangiogenesis and progression.[73,74] It was found that abnormal expression of ITGA9 in a variety of tumors was closely related to the proliferation, metastasis, adhesion of tumor cells, and angiogenesis.[75] ITGAV and ITGAM are associated with immune checkpoint blockade.[76,77]

Other alleged mechanisms responsible for cell proliferation and survival of lymphoma cells with n.29A/G in the *MIR142* gene in the CNS include loss of control over the following targets.

It has been proven that during the initiation and progression of DLBCL, a number of intracellular signaling pathways occur, including NF-kB, PI3K-AKT-mTOR, JAK-STAT, and MAPK. Genomic investigations indicate that several signaling pathways participate in the cell proliferation and survival of lymphoma cells in PCNSL, particularly constitutive NF-κB activation and deregulated TLR, BCR, PI3K-AKT-mTOR, and JAK-STAT pathways.[78] As a result of the mutation n.29A/G in the *MIR142* gene, there is a disruption in the targeting of miR-142-5p on a number of MAPK (MAP3K2, MAPK9, MAPK10) and PI3K-AKT-mTOR (PIK3CA, RICTOR) pathways, contributing to downstream NF-kB activation (TNFSF13B). In addition, there is a disruption in the targeting of miR-142-5p on main signaling molecules of the JAK-STAT signaling pathway (IL22, IL6ST), which allows tumor lymphocytes to survive in a poor growth-stimulus environment of the CNS.

In particular, TNFSF13B is a cytokine that activates the NF-κB transcription pathway and supports the survival of B cells. The interaction of TNFSF13B with its receptors contributes to both canonical and non-canonical signaling of NF-κB. TNFSF13B gene expression is also regulated by NF-κB through a positive feedback mechanism, promoting autocrine regulation of growth and survival. TNFRSF13B was significantly upregulated in ABC-DLBCL, and its high expression was associated with poor prognosis in DLBCL.[79,80]

Limitations

One of the limitations is the relatively small sample set size. There was no standardization by gender and age. This is due to the great rarity of the pathology. It accounts for less than 1% of all non-Hodgkin's lymphomas, and not all patients are suitable for stereotactic biopsy.[78] Future studies should confirm our findings by conducting larger-scale studies in multicenter sets of PCNSL samples. In addition, the instability of the pri-miR-142 hairpin and the change in the spectrum of target genes as a result of SNV predicted *in silico* need experimental validation. Functional wet-lab data are essential to confirm that the predicted structural/regulatory changes translate to biological effects in PCNSL cells. Besides, miR-142 expression is known to correlate with prognosis in systemic DLBCL.[20,21] Currently, there is no data on the prognostic value of *MIR142* mutations. Exploring associations between *MIR142* mutation status (presence/absence, specific SNVs) and clinical outcomes (e.g., survival, treatment response, relapse risk) in PCNSL patients in large patient samples is needed in future studies.

Conclusions

The mutation frequency in *MIR142* in a set of 35 primary DLBCL of the CNS samples was 37.1%. It exceeds the data for systemic DLBCL. Moreover, multiple single-nucleotide substitutions occurred in every third case, which indirectly indicates the possibility of the kataegis phenomenon in the region of this gene location. Overall, the obtained results indicate the fragility of the pri-miR-142 hairpin. SNVs located outside the seed sequence are capable of disrupting the stability and secondary organization of the pri-miR-142 hairpin, as well as facilitating the switching of target genes of the mature chains of the studied miRNA. Further functional studies are required to validate the obtained data and to confirm the impact of the predicted changes in thermodynamic stability and hairpin structure on the biogenesis and functional properties of mature miRNA chains. The high frequency of mutations in the gene in PCNS that we have identified is encouraging regarding their potential clinical usefulness and requires additional research effort.

Acknowledgments

None.

Funding

The work was funded by the Russian Science Foundation grant No. 25-25-00068.

Conflict of interest

The authors declare that the research was conducted in the absence of any commercial or financial relationships that could be construed as a potential conflict of interest.

Author contributions

Conceptualization (EV, VM, TP), methodology (EV, OS, VM, TP), software (YO), investigation (EV, OS, MV, TB), formal analysis (MV, TB), writing – original draft (EV, OS), writing – review & editing (MV, TB, VM, YO, TP), visualization (EV, OS, YO), project administration (VM, TP), and supervision (VM, TP). All authors have approved the final version and publication of the manuscript.

Ethical statement

The study was approved by the Bioethics Committee of Novosibirsk State Medical University (№129 from November 30, 2020) and was conducted in compliance with the Declaration of Helsinki (as revised in 2024). Written informed consent was obtained from all study participants. DNAs were extracted by the phenol-chloroform method with guanidine.

Data sharing statement

The data on enrichment of Gene Ontology terms of biological processes for miR-142-5p target gene lists (Supplementary Fig. 1) and predicted secondary structures of the microRNA hairpin (Supplementary Fig. 2) used to support the findings of this study are included within the supplementary information files.

References

[1] Voropaeva EN, Karpova VS, Pospelova TI, Maksimov VN, Vorontsova EV. Current research on the role of the blood-brain barrier in the central nervous system lymphomas development. J Siberian Med Sci 2022;6(2):131–147. doi:10.31549/2542-1174-2022-6-2-131-147.

[2] Pospelova TI, Voropaeva E, Karpova VS, Nechunaeva IN, Rzaev DA, Stupak VV, *et al*. Title of the article. J Siberian Med Sci 2024;6(4):112–132. doi:10.31549/2542-1174-2022-6-4-112-132.

[3] Louis DN, Perry A, Wesseling P, Brat DJ, Cree IA, Figarella-Branger D, *et al*. The 2021 WHO Classification of Tumors of the Central Nervous System: a summary. Neuro Oncol 2021;23(8):1231–1251. doi:10.1093/neuonc/noab106, PMID:34185076.

[4] Montesinos-Rongen M, Schmitz R, Courts C, Stenzel W, Bechtel D, Niedobitek G, Blümcke I, Reifenberger G, von Deimling A, Jungnickel B, Wiestler OD, Küppers R, Deckert M. Absence of immunoglobulin class switch in primary lymphomas of the central nervous system. Am J Pathol 2005;166(6):1773–9. doi:10.1016/S0002-9440(10)62487-X, PMID:15920162.

[5] Ferreri AJM, Calimeri T, Cwynarski K, Dietrich J, Grommes C, Hoang-Xuan K, *et al*. Primary central nervous system lymphoma. Nat Rev Dis Primers 2023;9(1):29. doi:10.1038/s41572-023-00439-0, PMID:37322012.

[6] O'Neill BP, Decker PA, Tieu C, Cerhan JR. The changing incidence of primary central nervous system lymphoma is driven primarily by the changing incidence in young and middle-aged men and differs from time trends in systemic diffuse large B-cell non-Hodgkin's lymphoma. Am J Hematol 2013;88(12):997–1000. doi:10.1002/ajh.23551, PMID:23873804.

[7] Villano JL, Koshy M, Shaikh H, Dolecek TA, McCarthy BJ. Age, gender, and racial differences in incidence and survival in primary CNS lymphoma. Br J Cancer 2011;105(9):1414–1418. doi:10.1038/bjc.2011.357, PMID:21915121.

[8] Royer-Perron L, Hoang-Xuan K, Alentorn A. Primary central nervous system lymphoma: time for diagnostic biomarkers and biotherapies? Curr Opin Neurol 2017;30(6):669–676. doi:10.1097/WCO.0000000000000492, PMID:28922238.

[9] Voropaeva EN, Pospelova TI, Karpova VS, Churkina MI, Vyatkin YuV, Ageeva TA, *et al*. Mutation profile of diffuse large B-cell lymphoma with relapses in the central nervous system. Adv Mol Oncol 2022;9(3):69–84. doi:10.17650/2313-805X-2022-9-3-69-84.

[10] Zheng X, Li P, Dong Q, Duan Y, Yang S, Cai Z, *et al*. MicroRNAs as Diagnostic Biomarkers in Primary Central Nervous System Lymphoma: A Systematic Review and Meta-Analysis. Front Oncol 2021;11:743542. doi:10.3389/fonc.2021.743542, PMID:34604087.

[11] Sebestyén E, Nagy Á, Marosvári D, Rajnai H, Kajtár B, Deák B, *et al*. Distinct miRNA Expression Signatures of Primary and Secondary Central Nervous System Lymphomas. J Mol Diagn 2022;24(3):224–240. doi:10.1016/j.jmoldx.2021.11.005, PMID:34954119.

[12] Voropaeva EN, Pospelova TI, Orlov YL, Churkina MI, Berezina OV, Gurazheva AA, *et al*. The Methylation of the p53 Targets the Genes MIR-203, MIR-129-2, MIR-34A and MIR-34B/C in the Tumor Tissue of Diffuse Large B-Cell Lymphoma. Genes (Basel) 2022;13(8):1401. doi:10.3390/genes13081401, PMID:36011313.

[13] Voropaeva EN, Orlov YL, Loginova AB, Seregina OB, Maksimov VN, Pospelova TI. Deregulation mechanisms and therapeutic opportunities of p53-responsive microRNAs in diffuse large B-cell lymphoma. PeerJ 2025;13:e18661. doi:10.7717/peerj.18661, PMID:39802185.

[14] Saliminejad K, Khorram Khorshid HR, Soleymani Fard S, Ghaffari SH. An overview of microRNAs: Biology, functions, therapeutics, and analysis methods. J Cell Physiol 2019;234(5):5451–5465. doi:10.1002/jcp.27486, PMID:30471116.

[15] Voropaeva EN, Seregina OB, Voytko MS, Babaeva TN, Skvortsova NV, Maksimov VN, *et al*. The significance of miR-142 in tumor progression of diffuse large B-cell lymphoma. Oncohematology 2025;20(2):87–103. doi:10.17650/1818-8346-2025-20-2-87-103.

[16] Lenze D, Leoncini L, Hummel M, Volinia S, Liu CG, Amato T, *et al*. The different epidemiologic subtypes of Burkitt lymphoma share a homogenous micro RNA profile distinct from diffuse large B-cell lymphoma. Leukemia 2011;25(12):1869–1876. doi:10.1038/leu.2011.156, PMID:21701491.

[17] Chen Y, Kincaid RP, Bastin K, Fachko DN, Skalsky RL. MicroRNA-focused CRISPR/Cas9 screen identifies miR-142 as a key regulator of Epstein-Barr virus reactivation. PLoS Pathog 2024;20(6):e1011970. doi:10.1371/journal.ppat.1011970, PMID:38885264.

[18] Ayoubian H, Ludwig N, Fehlmann T, Menegatti J, Gröger L, Anastasiadou E, *et al*. Epstein-Barr Virus Infection of Cell Lines Derived from Diffuse Large B-Cell Lymphomas Alters MicroRNA Loading of the Ago2 Complex. J Virol 2019;93(3):e01297–18. doi:10.1128/JVI.01297-18, PMID:30429351.

[19] Menegatti J, Nakel J, Stepanov YK, Caban KM, Ludwig N, Nord R, *et al*. Changes of Protein Expression after CRISPR/Cas9 Knockout of miRNA-142 in Cell Lines Derived from Diffuse Large B-Cell Lymphoma. Cancers (Basel) 2022;14(20):5031. doi:10.3390/cancers14205031, PMID:36291816.

[20] Lawrie CH, Chi J, Taylor S, Tramonti D, Ballabio E, Palazzo S, *et al*. Expression of microRNAs in diffuse large B cell lymphoma is associated with immunophenotype, survival and transformation from follicular lymphoma. J Cell Mol Med 2009;13(7):1248–1260. doi:10.1111/j.1582-4934.2008.00628.x, PMID:19413891.

[21] Bahashwan S, Alsaadi M, Barefah A, Almahdi H, Alahwal H, Almohammadi A, *et al*. Profiling of microRNAs by next-generation sequencing: Potential biomarkers for diffuse large B-cell lymphoma. J Taibah Univ Med Sci 2024;19(3):619–627. doi:10.1016/j.jtumed.2024.04.010, PMID:38812724.

[22] Kwanhian W, Lenze D, Alles J, Motsch N, Barth S, Döll C, *et al*. MicroRNA-142 is mutated in about 20% of diffuse large B-cell lymphoma. Cancer Med 2012;1(2):141–155. doi:10.1002/cam4.29, PMID:23342264.

[23] Hezaveh K, Kloetgen A, Bernhart SH, Mahapatra KD, Lenze D, Richter J, *et al*. Alterations of microRNA and microRNA-regulated messenger RNA expression in germinal center B-cell lymphomas determined by integrative sequencing analysis. Haematologica 2016;101(11):1380–1389. doi:10.3324/haematol.2016.143891, PMID:27390358.

[24] Morin RD, Assouline S, Alcaide M, Mohajeri A, Johnston RL, Chong L, *et al*. Genetic Landscapes of Relapsed and Refractory Diffuse Large B-Cell Lymphomas. Clin Cancer Res 2016;22(9):2290–2300. doi:10.1158/1078-0432.CCR-15-2123, PMID:26647218.

[25] Hornshøj H, Nielsen MM, Sinnott-Armstrong NA, Świtnicki MP, Juul M, Madsen T, *et al*. Pan-cancer screen for mutations in non-coding elements with conservation and cancer specificity reveals correlations with expression and survival. NPJ Genom Med 2018;3:1. doi:10.1038/s41525-017-0040-5, PMID:29354286.

[26] Khoury JD, Solary E, Abla O, Akkari Y, Alaggio R, Apperley JF, *et al*. The 5th edition of the World Health Organization Classification of Haematolymphoid Tumours: Myeloid and Histiocytic/Dendritic Neoplasms. Leukemia 2022;36(7):1703–1719. doi:10.1038/s41375-022-01613-1, PMID:35732831.

[27] Galka-Marciniak P, Kanduła Z, Tire A, Wegorek W, Gwozdz-Bak K, Handschuh L, *et al*. Mutations in the miR-142 gene are not common in myeloproliferative neoplasms. Sci Rep 2022;12(1):10924. doi:10.1038/s41598-022-15162-1, PMID:35764886.

[28] Hart RK, Fokkema IFAC, DiStefano M, Hastings R, Laros JFJ, Taylor R, *et al*. HGVS Nomenclature 2024: improvements to community engagement, usability, and computability. Genome Med 2024;16(1):149. doi:10.1186/s13073-024-01421-5, PMID:39702242.

[29] Kozomara A, Birgaoanu M, Griffiths-Jones S. miRBase: from microRNA sequences to function. Nucleic Acids Res 2019;47(D1):D155–D162. doi:10.1093/nar/gky1141, PMID:30423142.

[30] Chen Y, Wang X. miRDB: an online database for prediction of functional microRNA targets. Nucleic Acids Res 2020;48(D1):D127–D131. doi:10.1093/nar/gkz757, PMID:31504780.

[31] Thomas PD, Ebert D, Muruganujan A, Mushayahama T, Albou LP, Mi

H. PANTHER: Making genome-scale phylogenetics accessible to all. Protein Sci 2022;31(1):8–22. doi:10.1002/pro.4218, PMID:34717010.
[32] Aleksander SA, Balhoff J, Carbon S, Cherry JM, Drabkin HJ, Ebert D, *et al*. The Gene Ontology knowledgebase in 2023. Genetics 2023;224(1):iyad031. doi:10.1093/genetics/iyad031, PMID:36866529.
[33] Huang W, Paul D, Calin GA, Bayraktar R. miR-142: A Master Regulator in Hematological Malignancies and Therapeutic Opportunities. Cells 2023;13(1):84. doi:10.3390/cells13010084, PMID:38201290.
[34] Ma H, Wu Y, Choi JG, Wu H. Lower and upper stem-single-stranded RNA junctions together determine the Drosha cleavage site. Proc Natl Acad Sci U S A 2013;110(51):20687–20692. doi:10.1073/pnas.1311639110, PMID:24297910.
[35] Puente XS, Beà S, Valdés-Mas R, Villamor N, Gutiérrez-Abril J, Martín-Subero JI, *et al*. Non-coding recurrent mutations in chronic lymphocytic leukaemia. Nature 2015;526(7574):519–524. doi:10.1038/nature14666, PMID:26200345.
[36] Ley TJ, Miller C, Ding L, Raphael BJ, Mungall AJ, Robertson A, *et al*. Genomic and epigenomic landscapes of adult de novo acute myeloid leukemia. N Engl J Med 2013;368(22):2059–2074. doi:10.1056/NEJMoa1301689, PMID:23634996.
[37] Thol F, Scherr M, Kirchner A, Shahswar R, Battmer K, Kade S, *et al*. Clinical and functional implications of microRNA mutations in a cohort of 935 patients with myelodysplastic syndromes and acute myeloid leukemia. Haematologica 2015;100(4):e122–e124. doi:10.3324/haematol.2014.120345, PMID:25552704.
[38] Bouska A, Zhang W, Gong Q, Iqbal J, Scuto A, Vose J, *et al*. Combined copy number and mutation analysis identifies oncogenic pathways associated with transformation of follicular lymphoma. Leukemia 2017;31(1):83–91. doi:10.1038/leu.2016.175, PMID:27389057.
[39] Radke J, Ishaque N, Koll R, Gu Z, Schumann E, Sieverling L, *et al*. The genomic and transcriptional landscape of primary central nervous system lymphoma. Nat Commun 2022;13(1):2558. doi:10.1038/s41467-022-30050-y, PMID:35538064.
[40] Veerla S, Staaf J. Kataegis in clinical and molecular subgroups of primary breast cancer. NPJ Breast Cancer 2024;10(1):32. doi:10.1038/s41523-024-00640-8, PMID:38658600.
[41] Casellas R, Basu U, Yewdell WT, Chaudhuri J, Robbiani DF, Di Noia JM. Mutations, kataegis and translocations in B cells: understanding AID promiscuous activity. Nat Rev Immunol 2016;16(3):164–176. doi:10.1038/nri.2016.2, PMID:26898111.
[42] Marshall A, Kasturiarachchi J, Datta P, Guo Y, Deltcheva E, James C, *et al*. Mir142 loss unlocks IDH2(R140)-dependent leukemogenesis through antagonistic regulation of HOX genes. Sci Rep 2020;10(1):19390. doi:10.1038/s41598-020-76218-8, PMID:33173219.
[43] Urbanek-Trzeciak MO, Galka-Marciniak P, Nawrocka PM, Kowal E, Szwec S, Giefing M, *et al*. Pan-cancer analysis of somatic mutations in miRNA genes. EBioMedicine 2020;61:103051. doi:10.1016/j.ebiom.2020.103051, PMID:33038763.
[44] Pawlina-Tyszko K, Semik-Gurgul E, Gurgul A, Oczkowicz M, Szmatoła T, Bugno-Poniewierska M. Application of the targeted sequencing approach reveals the single nucleotide polymorphism (SNP) repertoire in microRNA genes in the pig genome. Sci Rep 2021;11(1):9848. doi:10.1038/s41598-021-89363-5, PMID:33972633.
[45] Mildner A, Chapnik E, Varol D, Aychek T, Lampl N, Rivkin N, *et al*. MicroRNA-142 controls thymocyte proliferation. Eur J Immunol 2017;47(7):1142–1152. doi:10.1002/eji.201746987, PMID:28471480.
[46] Busseau I, Mockly S, Houbron É, Somaï H, Seitz H. Evaluation of microRNA variant maturation prior to genome edition. Biochimie 2024;217:86–94. doi:10.1016/j.biochi.2023.06.007, PMID:37385398.
[47] Jouravleva K, Vega-Badillo J, Zamore PD. Principles and pitfalls of high-throughput analysis of microRNA-binding thermodynamics and kinetics by RNA Bind-n-Seq. Cell Rep Methods 2022;2(3):100185. doi:10.1016/j.crmeth.2022.100185, PMID:35475222.
[48] Gong J, Tong Y, Zhang HM, Wang K, Hu T, Shan G, *et al*. Genome-wide identification of SNPs in microRNA genes and the SNP effects on microRNA target binding and biogenesis. Hum Mutat 2012;33(1):254–263. doi:10.1002/humu.21641, PMID:22045659.
[49] Sheng P, Flood KA, Xie M. Short Hairpin RNAs for Strand-Specific Small Interfering RNA Production. Front Bioeng Biotechnol 2020;8:940. doi:10.3389/fbioe.2020.00940, PMID:32850763.
[50] Medley JC, Zinovyeva A. In silico unwinding of Caenorhabditis elegans microRNA duplexes to evaluate thermodynamic end stabilities improves predictions of microRNA strand selection. RNA Biol 2026;23(1):1–18. doi:10.1080/15476286.2026.2649359, PMID:41873897.
[51] Khvorova A, Reynolds A, Jayasena SD. Functional siRNAs and miRNAs exhibit strand bias. Cell 2003;115(2):209–216. doi:10.1016/s0092-8674(03)00801-8, PMID:14567918.
[52] Schwarzenbach H, Nishida N, Calin GA, Pantel K. Clinical relevance of circulating cell-free microRNAs in cancer. Nat Rev Clin Oncol 2014;11(3):145–156. doi:10.1038/nrclinonc.2014.5, PMID:24492836.
[53] Trissal MC, Wong TN, Yao JC, Ramaswamy R, Kuo I, Baty J, *et al*. MIR142 Loss-of-Function Mutations Derepress ASH1L to Increase HOXA Gene Expression and Promote Leukemogenesis. Cancer Res 2018;78(13):3510–3521. doi:10.1158/0008-5472.CAN-17-3592, PMID:29724719.
[54] Yin Z, Shen H, Gu CM, Zhang MQ, Liu Z, Huang J, *et al*. MiRNA-142-3P and FUS can be Sponged by Long Noncoding RNA DUBR to Promote Cell Proliferation in Acute Myeloid Leukemia. Front Mol Biosci 2021;8:754936. doi:10.3389/fmolb.2021.754936, PMID:34746238.
[55] Creugny A, Fender A, Pfeffer S. Regulation of primary microRNA processing. FEBS Lett 2018;592(12):1980–1996. doi:10.1002/1873-3468.13067, PMID:29683487.
[56] Lewis BP, Burge CB, Bartel DP. Conserved seed pairing, often flanked by adenosines, indicates that thousands of human genes are microRNA targets. Cell 2005;120(1):15–20. doi:10.1016/j.cell.2004.12.035, PMID:15652477.
[57] Fukunaga R, Han BW, Hung JH, Xu J, Weng Z, Zamore PD. Dicer partner proteins tune the length of mature miRNAs in flies and mammals. Cell 2012;151(3):533–546. doi:10.1016/j.cell.2012.09.027, PMID:23063653.
[58] Wenzel SS, Grau M, Mavis C, Hailfinger S, Wolf A, Madle H, *et al*. MCL1 is deregulated in subgroups of diffuse large B-cell lymphoma. Leukemia 2013;27(6):1381–1390. doi:10.1038/leu.2012.367, PMID:23257783.
[59] Dewaele M, Tabaglio T, Willekens K, Bezzi M, Teo SX, Low DH, *et al*. Antisense oligonucleotide-mediated MDM4 exon 6 skipping impairs tumor growth. J Clin Invest 2016;126(1):68–84. doi:10.1172/JCI82534, PMID:26595814.
[60] Skoufos G, Kakoulidis P, Tastsoglou S, Zacharopoulou E, Kotsira V, Miliotis M, *et al*. TarBase-v9.0 extends experimentally supported miRNA-gene interactions to cell-types and virally encoded miRNAs. Nucleic Acids Res 2024;52(D1):D304–D310. doi:10.1093/nar/gkad1071, PMID:37986224.
[61] Kiliçarslan A, Kurt Çevik G, Doğan M, Aksoy Altinboğa A, Ceran F, Efecik G, *et al*. Does CD47 expression have prognostic significance in classical Hodgkin lymphoma? Turk J Med Sci 2025;55(1):203–208. doi:10.55730/1300-0144.5958, PMID:40104289.
[62] Zhang J, Jin S, Guo X, Qian W. Targeting the CD47-SIRPα signaling axis: current studies on B-cell lymphoma immunotherapy. J Int Med Res 2018;46(11):4418–4426. doi:10.1177/0300060518799612, PMID:30226089.
[63] Zhao P, Xie L, Yu L, Wang P. Targeting CD47-SIRPα axis for Hodgkin and non-Hodgkin lymphoma immunotherapy. Genes Dis 2024;11(1):205–217. doi:10.1016/j.gendis.2022.12.008, PMID:37588232.
[64] Shen YG, Ji MM, Yi HM, Shen R, Fu D, Cheng S, *et al*. CD47 overexpression is related to tumour-associated macrophage infiltration and diffuse large B-cell lymphoma progression. Clin Transl Med 2024;14(1):e1532. doi:10.1002/ctm2.1532, PMID:38193627.
[65] Geli CP, Medina-Gil D, Medina-Gil D, Hernandez C, Crespo M. Macrophages play a key role in controlling tumor growth and response to immunotherapy in primary central nervous system lymphoma. Blood 2023;142(Suppl 1):1642–1642. doi:10.1182/blood-2023-180719.
[66] Heming M, Haessner S, Wolbert J, Lu IN, Li X, Brokinkel B, *et al*. Intratumor heterogeneity and T cell exhaustion in primary CNS lymphoma. Genome Med 2022;14(1):109. doi:10.1186/s13073-022-01110-1, PMID:36153593.
[67] Cui T, Sun L, Guo X, Cheng C, Zhang N, Zhou S, *et al*. Tumor-derived CD109 orchestrates reprogramming of tumor-associated macrophages to dampen immune response. J Hepatol 2025;83(4):946–958. doi:10.1016/j.jhep.2025.03.035, PMID:40220905.

[68] de Charette M, Houot R. Hide or defend, the two strategies of lymphoma immune evasion: potential implications for immunotherapy. Haematologica 2018;103(8):1256–1268. doi:10.3324/haematol.2017.184192, PMID:30006449.
[69] Booman M, Douwes J, Glas AM, Riemersma SA, Jordanova ES, Kok K, *et al*. Mechanisms and effects of loss of human leukocyte antigen class II expression in immune-privileged site-associated B-cell lymphoma. Clin Cancer Res 2006;12(9):2698–2705. doi:10.1158/1078-0432.CCR-05-2617, PMID:16675561.
[70] Schwindt H, Vater I, Kreuz M, Montesinos-Rongen M, Brunn A, Richter J, *et al*. Chromosomal imbalances and partial uniparental disomies in primary central nervous system lymphoma. Leukemia 2009;23(10):1875–1884. doi:10.1038/leu.2009.120, PMID:19494841.
[71] El Hussein S, Shaw KRM, Vega F. Evolving insights into the genomic complexity and immune landscape of diffuse large B-cell lymphoma: opportunities for novel biomarkers. Mod Pathol 2020;33(12):2422–2436. doi:10.1038/s41379-020-0616-y, PMID:32620919.
[72] Waldera-Lupa DM, Poschmann G, Kirchgaessler N, Etemad-Parishanzadeh O, Baberg F, Brocksieper M, *et al*. A Multiplex Assay for the Stratification of Patients with Primary Central Nervous System Lymphoma Using Targeted Mass Spectrometry. Cancers (Basel) 2020;12(7):1732. doi:10.3390/cancers12071732, PMID:32610669.
[73] Tang YL, Li GS, Li DM, Tang D, Huang JZ, Feng H, *et al*. The clinical significance of integrin subunit alpha V in cancers: from small cell lung carcinoma to pan-cancer. BMC Pulm Med 2022;22(1):300. doi:10.1186/s12890-022-02095-8, PMID:35927660.
[74] Su H, Wang J, Cao X, Zhang X, Zhang H, Liu X. ITGAV as a promising diagnostic, immunological, and prognostic biomarker in pan-cancer. Sci Rep 2025;15(1):28942. doi:10.1038/s41598-025-11836-8, PMID:40775249.
[75] Wu Y, Chen J, Tan F, Wang B, Xu W, Yuan C. ITGA9: Potential Biomarkers and Therapeutic Targets in Different Tumors. Curr Pharm Des 2022;28(17):1412–1418. doi:10.2174/1381612828666220501165644, PMID:35490433.
[76] Xia Y, Sun T, Li G, Li M, Wang D, Su X, *et al*. Spatial single cell analysis of tumor microenvironment remodeling pattern in primary central nervous system lymphoma. Leukemia 2023;37(7):1499–1510. doi:10.1038/s41375-023-01908-x, PMID:37120690.
[77] Tan Z, Zhang Z, Yu K, Yang H, Liang H, Lu T, *et al*. Integrin subunit alpha V is a potent prognostic biomarker associated with immune infiltration in lower-grade glioma. Front Neurol 2022;13:964590. doi:10.3389/fneur.2022.964590, PMID:36388191.
[78] Jiang H, Nong L. The Landscape of Primary Central Nervous System Lymphoma (PCNSL): Clinicopathologic and Genomic Characteristics and Therapeutic Perspectives. Cancers (Basel) 2025;17(17):2909. doi:10.3390/cancers17172909, PMID:40941006.
[79] Sheng L, Li T, Li Y, Zhou M, Wang J, Lai Y, *et al*. Prognostic and immunological characterization of diffuse large B-cell lymphoma evaluated by co-stimulatory molecular-related features. Heliyon 2023;9(9):e19342. doi:10.1016/j.heliyon.2023.e19342, PMID:37809743.
[80] Zhang M, Xu-Monette ZY, Li L, Manyam GC, Visco C, Tzankov A, *et al*. RelA NF-κB subunit activation as a therapeutic target in diffuse large B-cell lymphoma. Aging (Albany NY) 2016;8(12):3321–3340. doi:10.18632/aging.101121, PMID:27941215.